Electronic Supplementary Material (ESI) for Physical Chemistry Chemical Physics.

Supporting Information for:

Kinetics and equilibrium constants of oligonucleotides at low concentrations. Hybridization and melting study.

Krzysztof Bielec[a†], Krzysztof Sozanski[a†], Marco Seynen[b], Zofia Dziekan[a], Pieter Rein ten Wolde[b], Robert Holyst[a*]

[a]Institute of Physical Chemistry, Polish Academy of Sciences, Kasprzaka 44/52, 01-224 Warsaw, Poland
[b] FOM Institute AMOLF, Science Park 104, 1098 XG Amsterdam, The Netherlands

† These authors contributed equally to this work.

* rholyst@ichf.edu.pl

1 FCS measurements for oligonucleotides in singlex and duplex forms

In the initial phase of the project, we studied carefully the purchased oligonucleotides using fluorescence correlation spectroscopy (FCS). Exemplary autocorrelation curves are shown in Figure S1. Hydrodynamic radii of oligonucleotides in both single-strand and duplex forms were calculated based on obtained diffusion coefficients at 25°C, according to Einstein-Smoluchowski equation. Hydrodynamic radii of labeled single strands of oligonucleotides are 1.4, 1.6 and 2.0 nm for 10, 13 and 20 base pairs, respectively. Upon duplex formation, these values changed to 1.4, 1.7, and 2.0 nm, respectively. Nevertheless, the differences in the radius between singlex and duplex forms are of the order of 10%. Such moderate difference precludes quantitative estimation of the bound fraction on the basis of FCS measurements. We mixed complementary strands and observed same sample in time intervals. Statistically at concentration 10 nM of oligonucleotides in confocal volume we observing both bounded and unbounded fraction, (ratio is 0.4 and 0.6 at equilibrium, 10 mM PB, Fig.8 A in the manuscript) that are recorded and analysed through correlation function. We compared the FCS data with FRET measurements of the same sample. FCS data did not showed significant change of diffusion coefficient, whereas FRET proved to be reliable. Therefore we focused on FRET as a primary technique throughout research.

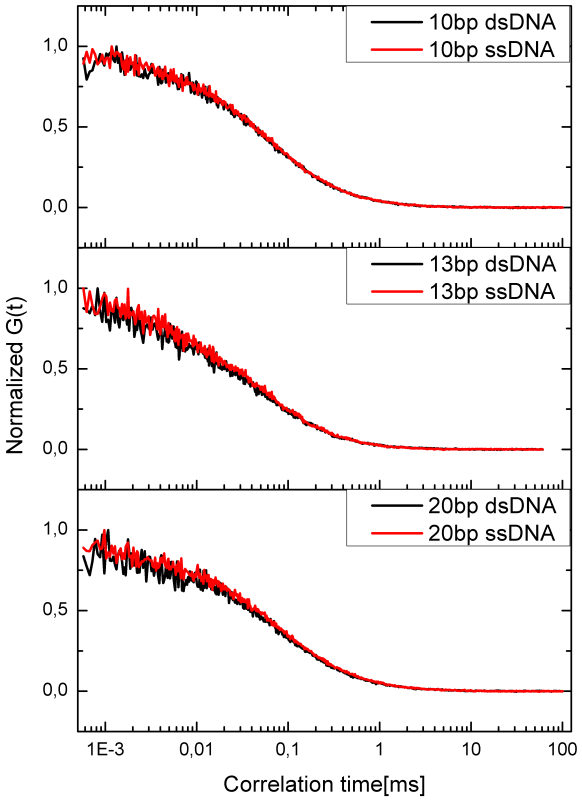

Fig S1. Autocorrelation function of purchased 10, 13 and 20 base pairs oligonucleotides, both in singlex and duplex forms. According to obtained diffusion times diffusion coefficient of singlex forms were 174, 154 and 122 $\mu m^2/s$ oligonucleotides. Fully bounded duplexes diffusion coefficients changed to 173, 144 and 122 $\mu m^2/s$, respectively.

2 Inffulence of coverglass surface passivation and addition of Tween 20 on oligonucletide concentration.

Sample hydrophilicity is a key factor influencing the surface adsorbtion, which affects bulk concentration and precludes quantitative studies, especially in case of low concentrations (nanomolar range and below). Aiming to minimize this effect, we tested two approaches: coverglass pasivation with PEG and addition of surfactant (Tween 20) to the solution. First, we diluted the oligonucleotide with pure PBS to concentration of 10 nM and poured it into a regular LabTek chambered coverglass container. The oligonucleotide measured therein by FCS was only 1.7 nM. Figure S2 shows that concentration of the oligonucleotide increased about ten times after addition of Tween 20 reaching 11.4 nM. In an experiment with surface modification, but no surfactant added, the measured concentration was 3.2 nM. However, a result of a combination of the two methods effect was similar to only surfactant addition itself. Furthermore, we did not observe any changes in the time of the diffusion with the presence of the Tween 20, as shown in the subplot of the Figure S2. Therefore, we included the addition of Tween 20 to the buffer in the standard experimental protocol for all experiments included in this study.

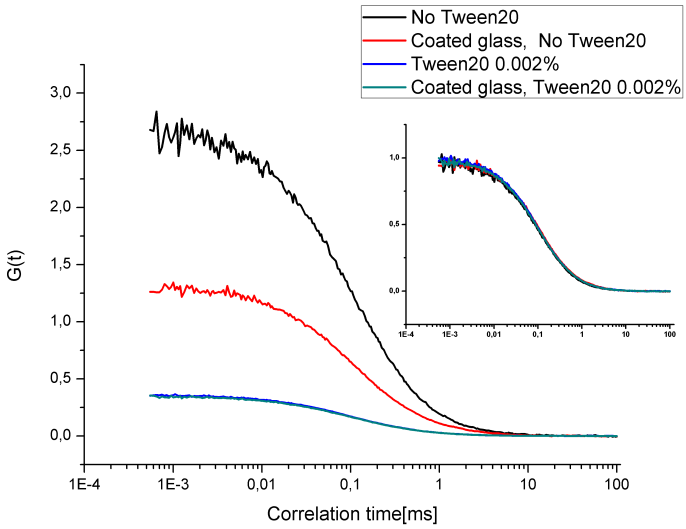

Fig S2. Fraction of bound (duplexed) oligonucleotides after 24 hours of incubation in pure 3 mM PB buffer and same buffer supplemented with Tween 20 at concentrations of 0.002%, 0.02% and 0.2%.

3 Influence of Tween 20 on the oligonucleotide binding equilibrium

Unless stated otherwise, all the experiments described in the paper were performed using solutions containing 0.002% Tween 20 surfactant to discourage oligonucleotide adsorption on the measurement chamber walls and the sample surface. To control whether the introduction of the surfactant may bias the results by introducing some stabilizing effect on the duplex, we performed a series of experiments where we diluted a fully duplexed 13 bp strand to final concentrations of 0.1, 1, and 10 nM in pure 3 mM PB buffer containing various amounts of added Tween 20. We measured the bound fraction using FRET after 24 hours of incubation at 25°C. The results are presented in Figure S3. Neither the normally used 0.002% surfactant addition, nor a 10 times greater amount of surfactant influenced the observed bound fraction values. For 0.2% Tween 20, we noted nearly complete dissolution of the duplexes. Also, for this high surfactant content samples, we observed large (hundreds of nm) objects in FCS measurements (data not shown). These objects are supramolecular structures formed by the surfactant. Due to the presence

of the hydrophobic dye, labeled oligonucleotides tend to adsorb on these objects, similarly to the case of phase boundaries. This seems to promote dissolution of the duplex, which is in line with the experiments where vigorous mixing was applied (see Section 4). However, the Tween 20 concentration of 0.002%, normally used in this work, is well below the critical micellization concentration of this surfactant of 0.006 %. [1] Therefore, no interference from supramolecular entities is expected.

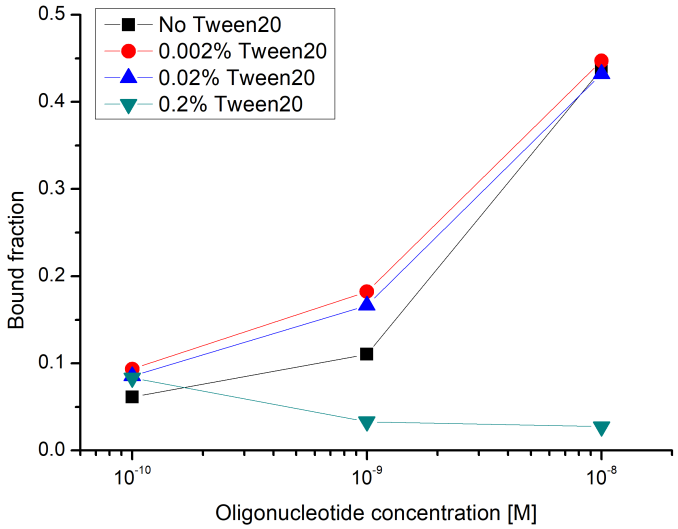

Fig S3. Fraction of bound (duplexed) oligonucleotides after 24 hours of incubation in pure 3 mM PB buffer and same buffer supplemented with Tween 20 at concentrations of 0.002%, 0.02% and 0.2%.

4 Effect of excessive mixing of the reaction mixture

Addition of surfactant was necessary to keep the oligonucleotides from adsorbing on the container walls and sample/air interface. As described above, Tween 20 at concentrations below critical micellization concentration did not cause the formation of any supramolecular artifacts that could disturb the experiments. However, even at moderate concentration, the solutions are prone to mild foaming when vigorous shaking is applied. To assess the possible effects of such treatment on the oligonucleotide binding equilibrium, we performed tests where a batch of a fully bound duplex of 13 bp oligonucleotide was diluted to a concentration of 100 pM, gently stirred and then split into three batches. One was left to equilibrate at room temperature, one was vigorously shaken for 30 minutes using a micro-shaker in an Eppendorf tube, and one was mixed by hand for 30 minutes by continuously turning an Eppendorf tube upside down and back. Care was taken not to heat up the samples during mixing. The results are presented in Figure S4.

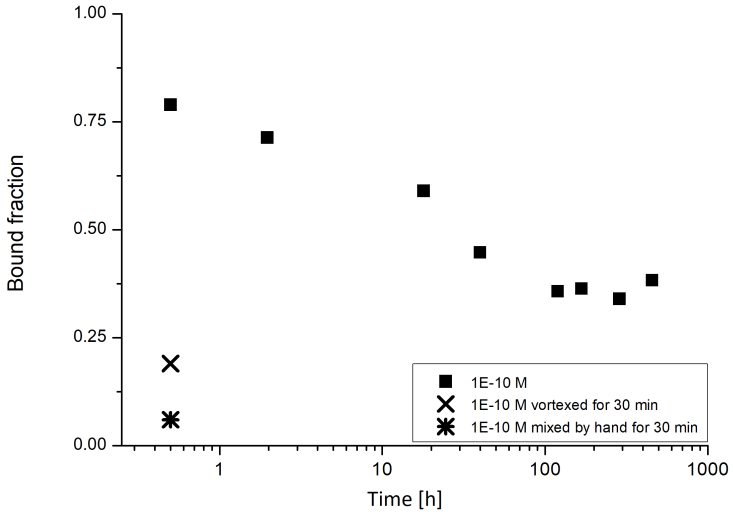

Fig S4. Bound fraction of a 13 bp oligonucleotide at 25°Cdiluted to 100 pM in 10 mM PB buffer with 0.002% Tween 20, observed for over a course of 1000 hours from the moment of diluting the 10 mM stock of fully-bound duplex to the target concentration. It takes days for the equilibrium to be reached. However, if the solution is mixed vigorously, the bound fraction drops well below the equilibrium value within less then 30 minutes.

In the sample that was not subject to mixing, it took over 100 hours to reach the equilibrium. At equilibrium conditions, the bound fraction was around 35%. In contrast, in both samples that were subject to vigorous mixing, already after 30 minutes the recorded bound fraction was well below the expected equilibrium value. We ascribe this result to foaming of the solutions during mixing. Due to the hydrophobic character of the fluorescent labels attached to the oligonucleotides, they tend to accumulate within the vast phase boundary surface available in the foam. Moreover, one of the labels (Atto 647N) presents stronger hydrophobic properties than the other (Atto 488). Apparently, in these conditions melting of the strands is promoted. We treated this information solely as a precaution to avoid excessive mixing and foaming during sample preparation. We did not look into the return of the system to equilibrium when foam settles,an influence of the presence of labels and their hydrophobicity on the process, or its molecular mechanism. However, we note that this may potentially be an interesting starting point for further investigation.

5 Experiments in 20 μL and 2mL vials

Double-strand 13 bp oligonucleotide stock was diluted to concentrations of 0.1, 1, and 10 nM in 2 mL of 10 mM PB buffer with 0.002% Tween 20. Immediately after the dilution, 20 uL of each of the three samples was placed on a separate coverglass. The remaining 1980 µL was kept as the "large volume" control. All samples were incubated at 20°C for 24 hours, in a water vapor saturated chamber (to prevent evaporation from the droplets). We performed 6 measurements for each sample during the incubation period. Irrespective of the oligonucleotide dilution or reaction progress, we noted no systematic differences between the bound fraction values measured in the 20 µL and 1980 µL incubation volumes.

6 eGFRD simulations

In order to sight the change in the effective rate constants k_+ and k_-, we performed simulations for a simple model reaction A + B $\rightleftarrows$ AB. Forward and backward intrinsic rates of binding given contact were set to $k_a = 6 \times 10^7$ $\mathrm{M}^{-1}\mathrm{s}^{-1}$ and $k_d = 0.1\mathrm{s}^{-1}$, respectively. The diffusion constant for all species was

$D = 1\mu\text{m}^2 s^{-1}$ and the cross-section of the A-B interaction was $\sigma = 2\text{nm}$. Simulation box initially contained 100 A molecules and 100 B molecules. Concentration was changed by changing the dimensions of the simulation box. Bound fraction for each concentration point, was obtained from 25 independent simulations. The enhanced Green's function reaction dynamics (eGFRD) algorithm uses Green's functions to analytically solve particle-particle interaction problems. Since the algorithm is driven by reaction events and the size of the diffusion step is flexible, it is highly efficient at molecular simulations of reaction-diffusion problems. In this case, it allowed us to confirm that even in the limit of extreme dilution of reagents, no effects related to reagent rebinding after dissociation should be expected that are not intrinsically included in the k_a and k_d definition.

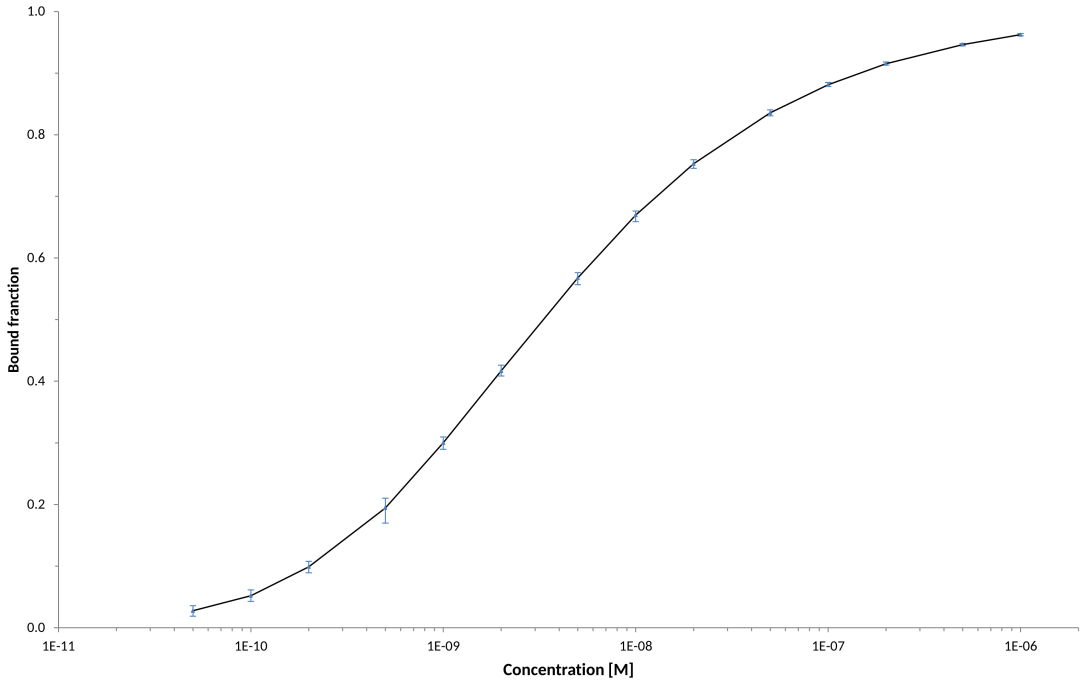

Fig S5. Bound fraction at equilibrium obtained from eGFRD simulations (data points) and expected on the basis of mean field calculations (solid curve) for various total reagent concentrations.

7 Determination of rate constants

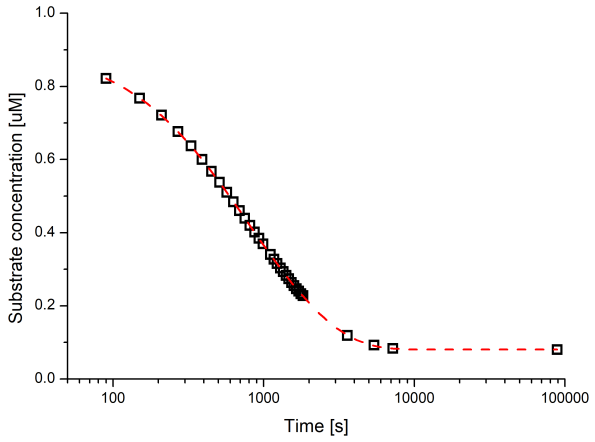

Fig S6. Exemplary data on progress of the hybridization reaction, starting from single strands. Substrate concentration at given time points was established on the basis of FRET measurements as described in the main text. This example concerns a complementary pair of 20 base long strands at 35℃ at concentration of 1 μM in a 3 mM PB buffer. Dashed line serves a a guide for the eye.

As described in the main text, k_+ was established by fitting the equation [2]

$$\ln\left(\frac{\delta_t}{\delta_t+\alpha}\right) = -k_+\alpha t + C, \tag{1}$$

where $\delta_t = [\mathrm{A}]_t - [\mathrm{A}]_{eq}$, $\alpha = 2[\mathrm{A}]_{eq} + K^{-1}$, t is the time from the moment of reaction initiation and C is a constant. An exemplary fit to experimental data from the previous figure is presented in the figure below.

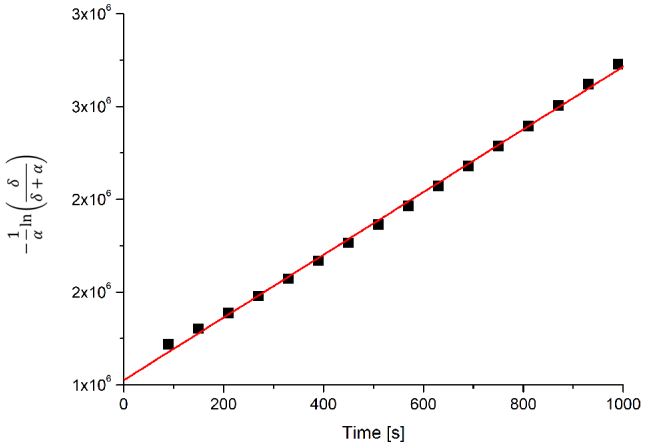

Fig S7. Exemplary curve used for of retrieving the rate constant from the change in reagent concentrations over time.

8 Label brightness changes upon hybridization

As described in the main text, in some experiments we used a pulsed interleaved excitation scheme where we independently monitored the fluorescence of the acceptor after its direct excitation. Interestingly, we noted that the brightness of the acceptor label changed significantly during the course of the reaction.

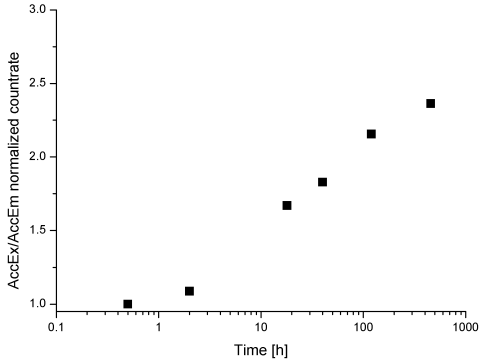

Fig S8. Changes in the number of photons per second recorded for acceptor emission channel after its direct excitation over the course of duplex melting reaction. Countrates are normalized to the value recorded at the first time point. This exemplary data concerns melting of a 13 base pair duplex diluted to 0.1 nM in 10 mM PB buffer and incubated at 25℃.

We performed additional fluorescence correlation spectroscopy analysis in parallel to the countrate analysis for acceptor direct excitation (data not shown). We found no change in total bulk concentration of the acceptor-labeled strand over time (information on concentration is retrieved from the amplitude of the autocorrelation function, which in principle does not depend on changes in the probe brightness nor size, i.e. it includes both single and double strand forms). To provide some insight into the photophysics behind the observed brightness changes, are influenced by the triplate state formation we performed FCS measurements. At the moderate laser power applied in all the experiments, we did not observe any triplet states for the acceptor dye. This remained true in all the performed controls: for free Atto 647N dye, for the dye bound to single-strand DNA, as well as for labeled oligonucleotide hybrydized with non-labeled and donor-labeled complementary strand. For all cases, autocorrelation curves could only be fitted by pure diffusion models, as shown in the Figure S9.

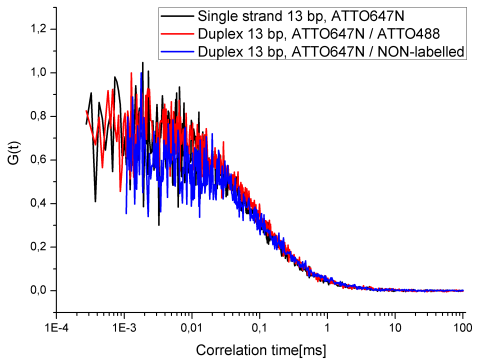

Fig S9. Autocorrelation curves from FCS measurements of single-strand DNA (acceptor) labeled with Atto 647N dye, double strand DNA (both acceptor and donor labeled by Atto 647N and ATTO488, respectively), double strand DNA (acceptor hybrydized with non-labeled complementary strand).

Also, we found that the acceptor brightness correlates well with the bound fraction. Therefore, we suspect that it is the change in the local environment of the acceptor dye caused by hybridization to the complementary strand that drives the shift in its brightness. We believe that this observation may be a basis for a promising method of reporting of strand binding, which would not require double labeling as traditional FRET does. We intend to investigate this topic further.

9 Summarized values for equilibrium constants, hybridization rates and melting rates

Table S1. Equilibrium constants, hybridization rates and melting rates presented in the Figure 9 in the manuscript.

		15°C		**25°C**		**35°C**	
		3 mM	**10 mM**	**3 mM**	**10 mM**	**3 mM**	**10 mM**
10 bp	$K_{eq}\left[\mathrm{M}^{-1}\right]$	$5{,}60{\cdot}10^{7}$	$1{,}71{\cdot}10^{9}$	$6{,}89{\cdot}10^{6}$	$7{,}50{\cdot}10^{7}$	$4{,}21{\cdot}10^{5}$	$4{,}45{\cdot}10^{6}$
	$k^{+}\left[\mathrm{M}^{-1}\mathrm{s}^{-1}\right]$	$8{,}31{\cdot}10^{3}$	$1{,}50{\cdot}10^{4}$	$8{,}97{\cdot}10^{3}$	$6{,}56{\cdot}10^{4}$	–	$1{,}13{\cdot}10^{5}$
	$k^{-}\left[\mathrm{s}^{-1}\right]$	$1{,}45{\cdot}10^{-4}$	$8{,}92{\cdot}10^{-6}$	$1{,}33{\cdot}10^{-3}$	$9{,}19{\cdot}10^{-4}$	–	$1{,}82{\cdot}10^{-2}$
13 bp	$K_{eq}\left[\mathrm{M}^{-1}\right]$	$1{,}04{\cdot}10^{8}$	$3{,}27{\cdot}10^{9}$	$5{,}23{\cdot}10^{7}$	$8{,}71{\cdot}10^{8}$	$6{,}84{\cdot}10^{6}$	$1{,}15{\cdot}10^{8}$
	$k^{+}\left[\mathrm{M}^{-1}\mathrm{s}^{-1}\right]$	$6{,}28{\cdot}10^{2}$	$1{,}31{\cdot}10^{4}$	$1{,}72{\cdot}10^{3}$	$2{,}53{\cdot}10^{4}$	–	$5{,}95{\cdot}10^{4}$
	$k^{-}\left[\mathrm{s}^{-1}\right]$	$4{,}22{\cdot}10^{-6}$	$6{,}19{\cdot}10^{-6}$	$3{,}30{\cdot}10^{-5}$	$3{,}07{\cdot}10^{-5}$	–	$5{,}68{\cdot}10^{-4}$
20 bp	$K_{eq}\left[\mathrm{M}^{-1}\right]$	$1{,}82{\cdot}10^{8}$	$7{,}36{\cdot}10^{9}$	$1{,}79{\cdot}10^{8}$	$3{,}57{\cdot}10^{9}$	$1{,}42{\cdot}10^{8}$	$1{,}46{\cdot}10^{9}$
	$k^{+}\left[\mathrm{M}^{-1}\mathrm{s}^{-1}\right]$	$6{,}35{\cdot}10^{2}$	$4{,}42{\cdot}10^{3}$	$6{,}61{\cdot}10^{2}$	$1{,}59{\cdot}10^{4}$	$2{,}09{\cdot}10^{3}$	$2{,}57{\cdot}10^{4}$
	$k^{-}\left[\mathrm{s}^{-1}\right]$	$3{,}46{\cdot}10^{-6}$	$6{,}13{\cdot}10^{-7}$	$3{,}69{\cdot}10^{-6}$	$5{,}60{\cdot}10^{-6}$	$8{,}40{\cdot}10^{-6}$	$2{,}00{\cdot}10^{-5}$

References

1. Helenius A, McCaslin DR, Fries E, Tanford C. Properties of detergents. vol. 56. Elsevier; 1979.
2. Esperson J. Chemical kinetics and reaction mechanism. McGraw-Hill Book Company: New York; 1981.